Research Square

Preprints are preliminary reports that have not undergone peer review.
They should not be considered conclusive, used to inform clinical practice,
or referenced by the media as validated information.

A Machine Learning-Based Model for Predicting Rhabdomyolysis in Patients With Sepsis

Xiangyi Zhou
First Affiliated Hospital of Chongqing Medical University
Hongbin Deng
Nanjing General Hospital of Nanjing Military Command
Daqian Gu
Nanjing General Hospital of Nanjing Military Command
Fachun Zhou
cyzfc1966@126.com

First Affiliated Hospital of Chongqing Medical University

Research Article

Keywords: Sepsis, Rhabdomyolysis, Machine Learning, Predictive Model, Intensive Care

Posted Date: December 10th, 2025

DOI: https://doi.org/10.21203/rs.3.rs-7904814/v1

License: This work is licensed under a Creative Commons Attribution 4.0 International License. Read Full License

Additional Declarations: No competing interests reported.

Abstract

Background

Sepsis is a common condition in the intensive care unit (ICU) and is frequently complicated by rhabdomyolysis, which can lead to serious consequences such as acute kidney injury. Currently, there is a lack of effective tools for the early prediction of sepsis-associated rhabdomyolysis.

Methods

This retrospective study analyzed 3,782 sepsis patients from the MIMIC-IV database. Three feature selection methods (multivariate analysis, LASSO regression, and the Boruta algorithm) were used to identify predictors. Six machine learning models (logistic regression, decision tree, random forest, XGBoost, support vector machine, and artificial neural network) were developed to predict the occurrence of rhabdomyolysis.

Results

Ten predictive features were ultimately identified. The XGBoost model demonstrated the best performance, achieving an area under the receiver operating characteristic curve (AUC) of 0.924 (95% CI: 0.907–0.941) in the validation set. SHAP analysis revealed that the CK/CKMB ratio, aspartate aminotransferase (AST), and invasive mechanical ventilation were the most important predictors.

Conclusions

The machine learning-based prediction model accurately identifies the risk of rhabdomyolysis in sepsis patients, facilitating the early recognition of high-risk individuals and enabling timely interventions.

Introduction

Sepsis remains a major cause of morbidity and mortality in the intensive care unit (ICU), characterized by dysregulated host response and multiple organ dysfunction[1]. Beyond its well-recognized complications, sepsis has been increasingly associated with skeletal muscle injury, particularly rhabdomyolysis[2,3]. Rhabdomyolysis is defined as the breakdown of skeletal muscle fibers with subsequent release of intracellular components such as creatine kinase, myoglobin, and electrolytes into the circulation, leading to severe metabolic disturbances, acute kidney injury, and worsened clinical outcomes[2,4]. Previous reports suggest that systemic inflammation, tissue hypoperfusion, mitochondrial dysfunction, and exposure to myo-/nephrotoxic agents may synergistically contribute to rhabdomyolysis in septic patients[2,5–7]. Despite its clinical significance, rhabdomyolysis in the context of critical illness is often challenging to recognize early because classic symptoms are nonspecific and creatine kinase elevation is typically detected after muscle injury has occurred[2,4].

Early identification of septic patients at risk of rhabdomyolysis is of critical importance for timely interventions, including optimized hemodynamic resuscitation, avoidance of myotoxic drugs, and early renal protection strategies[2,4]. Conventional diagnostic approaches rely mainly on elevated creatine kinase levels after muscle damage has occurred, which limits the potential for early preventive measures. Furthermore, rhabdomyolysis may develop insidiously in critically ill patients, making clinical suspicion and diagnosis challenging[4]. Therefore, a reliable predictive model could help clinicians stratify risk, monitor high-risk patients more closely, and implement targeted preventive strategies before irreversible muscle injury and secondary organ damage occur.

In recent years, machine learning techniques have shown great promise in healthcare by enabling the integration of large-scale, high-dimensional clinical data to generate accurate predictions and personalized risk assessments. Unlike traditional regression-based models, machine learning algorithms can capture complex nonlinear relationships and interactions among diverse clinical and laboratory variables, which are often present in sepsis pathophysiology[8–10]. Several machine learning-based models have already demonstrated superior performance in predicting complications such as acute kidney injury, septic shock, and mortality[8–13]. However, no predictive models specifically targeting sepsis-associated rhabdomyolysis have been systematically developed and validated to date. In this study, we aimed to construct and validate a machine learning-based predictive model for rhabdomyolysis in patients with sepsis using a large critical care database to provide clinicians with a practical tool for early risk stratification, thereby improving prevention and management strategies for this potentially life-threatening complication.

Methods

Data source and study population

This retrospective cohort study was conducted using data from the Medical Information Mart for Intensive Care IV (MIMIC-IV) database, a large, publicly available critical care database that contains detailed clinical information for patients admitted to the Beth Israel Deaconess Medical Center between 2008 and 2019. Access to the database was granted after completion of the required Collaborative Institutional Training Initiative course.

Adult patients (≥ 18 years) with an ICU stay longer than 24 hours were eligible. Sepsis was defined according to Sepsis-3 criteria, requiring suspected infection combined with a Sequential Organ Failure Assessment (SOFA) score ≥ 2. Exclusion criteria included: (1) history of acute myocardial infarction, congestive heart failure, advanced chronic kidney disease, chronic renal failure, chronic liver failure, dermatomyositis, or polymyositis; (2) absence of creatine kinase (CK) measurements; and (3) CK > 1000 U/L prior to sepsis diagnosis. For patients with multiple ICU admissions, only the first ICU stay was analyzed. The patient selection process is summarized in Fig. 1.

Outcome definition

The primary outcome was sepsis-associated rhabdomyolysis (RM), defined as serum CK level exceeding 1000 U/L after the onset of sepsis. Patients were classified into RM and non-RM groups accordingly.

Feature extraction and preprocessing

Demographic characteristics, comorbidities, vital signs, laboratory tests, severity scores (SOFA, SAPS II, APS III, OASIS, MELD, LODS, SIRS, GCS, Charlson Comorbidity Index), and treatment interventions (mechanical ventilation, cardiopulmonary resuscitation, continuous renal replacement therapy, renal replacement therapy) were extracted within the first 24 hours of ICU admission. Continuous variables were presented as medians with interquartile ranges, while categorical variables were presented as counts and percentages. Missing data were handled using multiple imputation with chained equations.

Feature selection

Three complementary methods were applied to identify robust predictors of RM: (1) multivariate logistic regression, selecting variables with $p < 0.05$; (2) least absolute shrinkage and selection operator (LASSO) regression with 10-fold cross-validation to minimize misclassification error; and (3) Boruta algorithm based on random forest importance scores. Features consistently identified by all three methods were considered final candidate predictors.

Model development and validation

The study cohort was randomly split into training (70%) and validation (30%) sets. Six machine learning algorithms were developed for RM prediction: logistic regression, decision tree, random forest, extreme gradient boosting (XGBoost), support vector machine (SVM), and artificial neural network (ANN). Hyperparameters were optimized through grid search with 5-fold cross-validation within the training set.

Model evaluation

Model performance was evaluated in the validation set using multiple metrics: area under the receiver operating characteristic curve (AUC), accuracy, sensitivity, specificity, precision, F1 score, kappa statistic, Youden's index, and positive and negative predictive values. Calibration curves with Brier scores and 95% confidence intervals were used to assess model calibration. Clinical utility was evaluated using decision curve analysis (DCA) (Fig. 3).

Model interpretation

To enhance interpretability, Shapley Additive Explanations (SHAP) analysis will be conducted on the model with the best performance. Global interpretability was assessed through mean absolute SHAP values and beeswarm plots, ranking the contribution of each predictor. Local interpretability was explored using waterfall plots to visualize the impact of individual features on the prediction for representative patients (Fig. 4).

Statistical analysis

Continuous variables were compared between groups using the Mann-Whitney U test, while categorical variables were compared using the chi-square or Fisher's exact test, as appropriate. All statistical analyses were performed using R (version 4.2.0) and Python (version 3.9). A two-sided p value < 0.05 was considered statistically significant.

Results

Patient selection

A total of 94,458 ICU admissions from the MIMIC-IV database were initially screened. After restricting to adult patients (≥ 18 years), with an ICU stay longer than 1 day, and fulfilling the Sepsis-3 criteria, 33,042 patients were eligible for further assessment. Patients with acute myocardial infarction (AMI), congestive heart failure (CHF), advanced chronic kidney disease (CKD stages 4–5), chronic renal failure (CRF), chronic liver failure (CLF), dermatomyositis (DM), or polymyositis (PM) were excluded. Subsequently, patients without peak CK measurements or with CK > 1000 U/L prior to the diagnosis of sepsis were also excluded. Finally, 3,782 patients were included in the analysis. The study cohort was randomly divided into a training set (70%) and an internal validation set (30%).

Baseline characteristics

A total of 3782 septic patients were included in the MIMIC-IV cohort, comprising 909 patients with rhabdomyolysis (RM group) and 2873 without rhabdomyolysis (non-RM group). Significant differences in demographic, clinical, and laboratory characteristics were observed between the two groups (Table 1).

Table 1
Baseline characteristics and comparison between RM and non-RM in MIMIC database

Demographic characteristics	Overall n = 3782	Non-RM n = 2873	RM n = 909	P value
Demographic information				
Male gender, n (%)	2148 [56.80]	1504 [52.35]	644 [70.85]	< 0.001
Age(yd)	65.00 [55.00, 75.00]	67.00 [57.00, 76.00]	58.00 [49.00, 69.00]	< 0.001
Height (cm)	170.00 [163.00, 178.00]	168.00 [163.00, 175.00]	173.00 [165.00, 178.00]	< 0.001
Weight (kg)	79.00 [67.00, 94.50]	77.20 [65.50, 92.30]	84.60 [71.90, 98.60]	< 0.001
BMI (kg/m^2)	27.47 [23.73, 32.03]	27.21 [23.44, 31.74]	28.41 [24.93, 32.86]	< 0.001
Los_hospital (d)	16.76 [9.60, 27.80]	17.96 [10.04, 29.28]	13.61 [7.56, 22.71]	< 0.001
Los_icu (d)	4.91 [2.44, 10.23]	4.67 [2.28, 9.84]	5.99 [2.84, 11.70]	< 0.001
Severity of illness				
AKI_score (median [IQR])	2.00 [2.00, 3.00]	2.00 [2.00, 3.00]	2.00 [2.00, 3.00]	0.005
Apsiii (median [IQR])	54.00 [42.00, 67.00]	54.00 [43.00, 67.00]	53.00 [40.00, 69.00]	0.542
SAPSii (median [IQR])	41.00 [33.00, 50.00]	41.00 [33.00, 49.00]	40.00 [31.00, 51.00]	0.266
SOFA (median [IQR])	7.00 [5.00, 11.00]	7.00 [5.00, 10.00]	8.00 [6.00, 12.00]	< 0.001
GCS (median [IQR])	13.00 [9.00, 14.00]	13.00 [10.00, 14.00]	13.00 [9.00, 14.00]	0.002
SIRS (median [IQR])	3.00 [2.00, 4.00]	3.00 [2.00, 3.00]	3.00 [3.00, 4.00]	< 0.001
LODS (median [IQR])	6.00 [4.00, 8.00]	6.00 [4.00, 8.00]	6.00 [4.00, 8.00]	< 0.001
Charlson (median [IQR])	5.00 [3.00, 7.00]	6.00 [4.00, 7.00]	3.00 [1.00, 6.00]	< 0.001
MELD (median [IQR])	17.58 [10.00, 24.68]	18.00 [11.00, 25.00]	16.57 [10.00, 24.00]	0.038
OASIS (median [IQR])	35.00 [30.00, 40.00]	35.00 [29.00, 40.00]	36.00 [31.00, 42.00]	< 0.001
Vital signs				< 0.001
Temperature (℃)	37.39 [37.00, 37.94]	37.28 [37.00, 37.83]	37.70 [37.20, 38.28]	0.002
HR (bpm)	109.00 [96.00, 122.00]	108.00 [96.00, 121.00]	111.00 [98.00, 122.00]	0.045
RR (bpm)	28.75 [25.00, 33.00]	29.00 [25.00, 33.00]	28.00 [24.00, 32.00]	< 0.001
SBP (mmHg)	144.00 [130.00, 158.00]	143.00 [129.00, 157.00]	146.00 [134.00, 162.00]	< 0.001
DBP (mmHg)	84.00 [73.00, 96.00]	84.00 [73.00, 96.00]	85.00 [76.00, 97.00]	< 0.001
MBP (mmHg)	99.75 [89.00, 112.00]	99.00 [88.00, 111.00]	103.00 [93.00, 116.00]	0.542
Laboratory fndings				
Spo2 (%)	100.00 [100.00, 100.00]	100.00 [100.00, 100.00]	100.00 [100.00, 100.00]	0.037
Calcium_free (mmol/L)	1.13 [1.08, 1.19]	1.13 [1.08, 1.19]	1.14 [1.08, 1.20]	0.007
WBC (K/uL)	12.70 [8.70, 17.80]	12.30 [8.30, 17.60]	13.50 [10.00, 18.40]	< 0.001
Hematocrit %	31.80 [28.20, 36.00]	30.90 [27.70, 34.80]	34.60 [31.10, 38.60]	< 0.001
MCH (pg)	30.50 [28.90, 31.90]	30.40 [28.70, 31.80]	30.70 [29.40, 32.00]	< 0.001

Data are shown as median with interquartile range (IQR) for continuous variables and number with percentage for categorical variables

SOFA: Sequential Organ Failure Assessment, SAPSII: Simplified Acute Physiology Score II, APSIII: Acute Physiology Score III, OASIS: Oxford Acute Severity of Illness Score, GCS: Glasgow Coma Scale, SIRS: Systemic Inflammatory Response Syndrome, LODS: Logistic Organ Dysfunction System, MELD: Model for End-Stage Liver Disease, Charlson: Charlson Comorbidity Index, RM: Rhabdomyolysis, BMI: Body Mass Index, HR: Heart Rate, RR: Respiratory Rate, SBP: Systolic Blood Pressure, DBP: Diastolic Blood Pressure, MBP: Mean Blood Pressure, SpO2: Oxygen Saturation, WBC: White Blood Cell, MCH: Mean Corpuscular Hemoglobin, MCV: Mean Corpuscular Volume, MCHC: Mean Corpuscular Hemoglobin Concentration, RDW: Red Cell Distribution Width, PLT: Platelet, RBC: Red Blood Cell, Alb: Albumin, BUN: Blood Urea Nitrogen, PT: Prothrombin Time, PTT: Partial Thromboplastin Time, INR: International Normalized Ratio, ALT: Alanine Aminotransferase, AST: Aspartate Aminotransferase, ALP: Alkaline Phosphatase, LDH: Lactate Dehydrogenase, Hb: Hemoglobin, AKI: Acute Kidney Injury, CPR: Cardiopulmonary Resuscitation, CRRT: Continuous Renal Replacement Therapy, RRT: Renal Replacement Therapy, IQR: Interquartile Range

Demographic characteristics	Overall n = 3782	Non-RM n = 2873	RM n = 909	P value
MCV (fL)	93.00 [88.00, 97.00]	93.00 [88.00, 98.00]	92.00 [88.00, 96.00]	0.005
MCHC (%)	33.20 [32.00, 34.30]	32.90 [31.90, 34.10]	33.90 [32.70, 34.90]	< 0.001
RDW (%)	15.60 [14.30, 17.10]	16.00 [14.60, 17.50]	14.70 [13.70, 15.60]	< 0.001
PLT (K/uL)	189.00 [125.00, 258.00]	190.00 [121.00, 261.00]	188.00 [139.00, 248.00]	0.451
RBC (m/uL)	3.48 [3.05, 3.98]	3.37 [2.97, 3.85]	3.80 [3.39, 4.26]	< 0.001
Alb (g/dl)	2.90 [2.60, 3.30]	2.90 [2.50, 3.30]	3.10 [2.70, 3.40]	< 0.001
Creatinine (mg/dl)	1.30 [0.90, 2.30]	1.30 [0.80, 2.20]	1.50 [1.00, 2.40]	< 0.001
BUN (mg/dl)	28.00 [17.00, 43.00]	29.00 [18.00, 45.00]	25.00 [16.00, 38.00]	< 0.001
Aniongap	16.00 [13.00, 19.00]	16.00 [13.00, 18.00]	17.00 [14.00, 20.00]	< 0.001
PT (seconds)	15.30 [13.30, 19.10]	15.50 [13.30, 19.50]	14.90 [13.00, 17.90]	< 0.001
PTT (seconds)	33.50 [28.70, 42.48]	33.70 [28.90, 42.30]	32.70 [28.30, 42.90]	0.139
INR	1.40 [1.20, 1.80]	1.40 [1.20, 1.80]	1.30 [1.20, 1.70]	< 0.001
CK_CKMB_ratio (U/L)	33.00 [14.00, 92.00]	23.00 [11.00, 54.00]	111.00 [57.00, 210.00]	< 0.001
ALT (U/L)	33.00 [18.00, 75.75]	29.00 [16.00, 60.00]	58.00 [29.00, 161.00]	< 0.001
AST (U/L)	50.00 [27.00, 120.00]	40.00 [24.00, 84.00]	117.00 [54.00, 335.00]	< 0.001
ALP (U/L)	88.00 [62.00, 133.00]	95.00 [67.00, 142.00]	66.00 [49.00, 95.00]	< 0.001
Bilirubin_total (mg/dl)	0.80 [0.40, 1.70]	0.80 [0.40, 1.80]	0.70 [0.40, 1.40]	< 0.001
LDH (U/L)	308.00 [218.00, 477.00]	277.00 [205.00, 408.00]	453.00 [302.00, 702.00]	< 0.001
Chloride (mg/dl)	106.00 [102.00, 110.00]	105.00 [101.00, 110.00]	108.00 [104.00, 112.00]	< 0.001
Glucose (mg/dl)	155.50 [121.00, 204.00]	150.00 [119.00, 198.00]	171.00 [132.00, 224.00]	< 0.001
Bicarbonate (g/dl)	24.00 [21.00, 26.00]	24.00 [21.00, 27.00]	23.00 [21.00, 26.00]	< 0.001
Hb (g/dl)	10.50 [9.20, 11.90]	10.10 [8.90, 11.40]	11.70 [10.40, 12.90]	< 0.001
K (mEq/L)	4.40 [4.00, 4.90]	4.30 [4.00, 4.80]	4.60 [4.10, 5.20]	< 0.001
Na (mEq/L)	140.00 [137.00, 143.00]	139.00 [136.00, 142.00]	141.00 [138.00, 144.00]	< 0.001
Mg (mg/dL)	2.20 [1.90, 2.40]	2.20 [1.90, 2.40]	2.20 [2.00, 2.50]	< 0.001
Ca(mg/dL)	8.40 [7.90, 8.80]	8.40 [7.90, 8.90]	8.30 [7.90, 8.70]	< 0.001
P (mg/dL)	4.10 [3.30, 5.10]	4.00 [3.20, 4.90]	4.40 [3.50, 5.40]	< 0.001
Input_24h_sum (ml)	4964.50 [2649.00, 8077.00]	4255.00 [2301.00, 7067.00]	7327.00 [4617.00, 10827.00]	< 0.001
Output_24h_sum (ml)	1860.00 [1050.00, 3033.75]	1770.00 [994.00, 2810.00]	2340.00 [1306.50, 3580.00]	< 0.001
Output_urine_sum (ml)	1302.50 [743.50, 2050.00]	1270.00 [729.00, 1975.00]	1430.00 [830.00, 2240.00]	< 0.001
Comorbidity, n (%)				
Smoker (%)	328 (8.67)	252 (8.77)	76 (8.36)	0.752

Data are shown as median with interquartile range (IQR) for continuous variables and number with percentage for categorical variables

SOFA: Sequential Organ Failure Assessment, SAPSII: Simplified Acute Physiology Score II, APSIII: Acute Physiology Score III, OASIS: Oxford Acute Severity of Illness Score, GCS: Glasgow Coma Scale, SIRS: Systemic Inflammatory Response Syndrome, LODS: Logistic Organ Dysfunction System, MELD: Model for End-Stage Liver Disease, Charlson: Charlson Comorbidity Index, RM: Rhabdomyolysis, BMI: Body Mass Index, HR: Heart Rate, RR: Respiratory Rate, SBP: Systolic Blood Pressure, DBP: Diastolic Blood Pressure, MBP: Mean Blood Pressure, SpO2: Oxygen Saturation, WBC: White Blood Cell, MCH: Mean Corpuscular Hemoglobin, MCV: Mean Corpuscular Volume, MCHC: Mean Corpuscular Hemoglobin Concentration, RDW: Red Cell Distribution Width, PLT: Platelet, RBC: Red Blood Cell, Alb: Albumin, BUN: Blood Urea Nitrogen, PT: Prothrombin Time, PTT: Partial Thromboplastin Time, INR: International Normalized Ratio, ALT: Alanine Aminotransferase, AST: Aspartate Aminotransferase, ALP: Alkaline Phosphatase, LDH: Lactate Dehydrogenase, Hb: Hemoglobin, AKI: Acute Kidney Injury, CPR: Cardiopulmonary Resuscitation, CRRT: Continuous Renal Replacement Therapy, RRT: Renal Replacement Therapy, IQR: Interquartile Range

Demographic characteristics	Overall n = 3782	Non-RM n = 2873	RM n = 909	P value
Alcohol_abuse (%)	59 (1.56)	41 (1.43)	18 (1.98)	0.308
Hypertension (%)	1391 (36.78)	1046 (36.41)	345 (37.95)	0.422
Diabetes (%)	1204 (31.84)	978 (34.04)	226 (24.86)	< 0.001
Myocardial_infarct (%)	279 (7.38)	224 (7.80)	55 (6.05)	0.092
Congestive_heart_failure (%)	1230 (32.52)	1026 (35.71)	204 (22.44)	< 0.001
Mild_liver_disease (%)	890 (23.53)	697 (24.26)	193 (21.23)	0.067
Severe_liver_disease (%)	472 (12.48)	426 (14.83)	46 (5.06)	< 0.001
Renal_disease (%)	1016 (26.86)	856 (29.79)	160 (17.60)	< 0.001
Chronic_pulmonary_disease (%)	1059 (28.00)	836 (29.10)	223 (24.53)	0.009
Cerebrovascular_disease (%)	550 (14.54)	405 (14.10)	145 (15.95)	0.184
Peripheral_vascular_disease (%)	504 (13.33)	373 (12.98)	131 (14.41)	0.294
Dementia (%)	123 (3.25)	105 (3.65)	18 (1.98)	0.018
Peptic_ulcer_disease (%)	162 (4.28)	140 (4.87)	22 (2.42)	0.002
Paraplegia (%)	197 (5.21)	146 (5.08)	51 (5.61)	0.589
Malignant_cancer (%)	578 (15.28)	509 (17.72)	69 (7.59)	< 0.001
Metastatic_solid_tumor (%)	179 (4.73)	151 (5.26)	28 (3.08)	0.009
Aids (%)	41 (1.08)	30 (1.04)	11 (1.21)	0.812
Rheumatic_disease (%)	171 (4.52)	144 (5.01)	27 (2.97)	0.013
AKI (%)	3224 (85.25)	2422 (84.30)	802 (88.23)	0.004
Treatment status				
InvasiveVent (%)	2348 (62.08)	1588 (55.27)	760 (83.61)	< 0.001
CPR (%)	76 (2.01)	45 (1.57)	31 (3.41)	0.001
CRRT (%)	555 (14.67)	363 (12.63)	192 (21.12)	< 0.001
RRT (%)	772 (20.41)	544 (18.93)	228 (25.08)	< 0.001

Data are shown as median with interquartile range (IQR) for continuous variables and number with percentage for categorical variables

SOFA: Sequential Organ Failure Assessment, SAPSII: Simplified Acute Physiology Score II, APSIII: Acute Physiology Score III, OASIS: Oxford Acute Severity of Illness Score, GCS: Glasgow Coma Scale, SIRS: Systemic Inflammatory Response Syndrome, LODS: Logistic Organ Dysfunction System, MELD: Model for End-Stage Liver Disease, Charlson: Charlson Comorbidity Index, RM: Rhabdomyolysis, BMI: Body Mass Index, HR: Heart Rate, RR: Respiratory Rate, SBP: Systolic Blood Pressure, DBP: Diastolic Blood Pressure, MBP: Mean Blood Pressure, SpO2: Oxygen Saturation, WBC: White Blood Cell, MCH: Mean Corpuscular Hemoglobin, MCV: Mean Corpuscular Volume, MCHC: Mean Corpuscular Hemoglobin Concentration, RDW: Red Cell Distribution Width, PLT: Platelet, RBC: Red Blood Cell, Alb: Albumin, BUN: Blood Urea Nitrogen, PT: Prothrombin Time, PTT: Partial Thromboplastin Time, INR: International Normalized Ratio, ALT: Alanine Aminotransferase, AST: Aspartate Aminotransferase, ALP: Alkaline Phosphatase, LDH: Lactate Dehydrogenase, Hb: Hemoglobin, AKI: Acute Kidney Injury, CPR: Cardiopulmonary Resuscitation, CRRT: Continuous Renal Replacement Therapy, RRT: Renal Replacement Therapy, IQR: Interquartile Range

Patients in the RM group were younger, more frequently male, and had higher body weight and body mass index compared with the non-RM group (all $p < 0.001$). Although hospital length of stay was shorter in the RM group, ICU length of stay was significantly longer (both $p < 0.001$). Regarding disease severity, RM patients had higher SOFA, SIRS, LODS, and OASIS scores, while Charlson Comorbidity Index was lower ($p < 0.001$).

RM patients presented with higher temperature, heart rate, and blood pressure levels. Laboratory findings revealed substantial differences between groups. The RM group showed significantly higher white blood cell counts, hematocrit, creatinine, anion gap, liver enzymes (ALT, AST), LDH, glucose, potassium, and phosphorus levels, whereas platelet counts and bilirubin were lower. CK/CKMB ratio was markedly elevated in the RM group (111.00 [57.00–210.00] vs. 23.00 [11.00–54.00], $p < 0.001$).

Compared with the non-RM group, RM patients had lower prevalence of diabetes, congestive heart failure, severe liver disease, and renal disease, but higher prevalence of acute kidney injury (88.23% vs. 84.30%, $p = 0.004$). In terms of treatment, invasive mechanical ventilation (InvasiveVent), cardiopulmonary resuscitation (CPR), continuous renal replacement therapy (CRRT), and renal replacement therapy (RRT) were all more frequently used in the RM group (all $p < 0.001$).

Feature selection

To identify robust predictors of sepsis-associated rhabdomyolysis, three complementary feature selection methods were applied: multivariate analysis, LASSO regression, and the Boruta algorithm (Fig. 2).

In the LASSO regression with 10-fold cross-validation, the misclassification error across different values of the tuning parameter was evaluated. The two vertical dashed lines indicate the optimal lambda values under the minimum and 1-standard error (SE) criteria, respectively. Using this approach, a total of 33 variables with non-zero coefficients were retained (Fig. 2A-B). The Boruta algorithm further ranked variable importance by comparing each feature with shadow features. Among all candidates, 22 variables were identified as important, while others were classified as neutral or rejected (Fig. 2C-D).

The intersection of the three approaches yielded 10 overlapping predictors that were consistently associated with rhabdomyolysis, common variables are provided in the supplementary file. These variables were selected as the final candidate predictors for subsequent model construction (Fig. 2E).

Model performance in the validation set

The predictive performance of six machine learning models-including logistic regression, decision tree, random forest, XGBoost, SVM, and ANN-was comprehensively evaluated in the validation set (Fig. 3).

Calibration analysis demonstrated that all models exhibited acceptable agreement between predicted and observed probabilities, with XGBoost and random forest showing the closest alignment to the ideal reference line and the lowest Brier scores (Fig. 3A). DCA further revealed that machine learning models, particularly XGBoost and random forest, provided greater net clinical benefit across a wide range of threshold probabilities compared with the strategies of treating all or treating none (Fig. 3B).

Receiver operating characteristic curves confirmed the superior discriminative performance of XGBoost, with the highest AUC, followed by random forest and ANN. Logistic regression and decision tree showed moderate discrimination, whereas SVM achieved good specificity but relatively lower sensitivity (Fig. 3C). The parameters of each model are provided in the supplementary file. Collectively, these results indicated that ensemble-based models, especially XGBoost, outperformed other approaches in predicting sepsis-associated rhabdomyolysis, The detailed performance metrics of all models in the validation set are presented in Table 2.

Table 2
Performance of 6 machine learning-based models for predicting ICU admission in the validation set

Model	AUC	95% CI Lower	95% CI Upper	Accuracy	Precision	Sensitivity	Specificity	F1 Score	Kappa	Youden's J	PPV	NPV
Logistic	0.877	0.856	0.898	0.826	0.712	0.463	0.941	0.561	0.459	0.404	0.712	0.847
Decision Tree	0.886	0.864	0.907	0.853	0.709	0.662	0.914	0.684	0.589	0.576	0.709	0.895
Random Forest	0.911	0.891	0.930	0.876	0.799	0.643	0.949	0.713	0.635	0.592	0.799	0.894
XGBoost	0.924	0.907	0.941	0.883	0.791	0.695	0.942	0.740	0.664	0.637	0.791	0.907
SVM	0.885	0.866	0.905	0.825	0.720	0.445	0.945	0.550	0.449	0.390	0.720	0.844
ANN	0.911	0.893	0.929	0.865	0.772	0.621	0.942	0.688	0.603	0.563	0.772	0.887

AUC: area under the receiver operating characteristic curve; XGBoost: eXtreme gradient boosting; SVM: Support Vector Machine; ANN: Artificial Neural Network

Model interpretation with SHAP analysis

To enhance the interpretability of the best-performing model, SHAP analysis was applied to the XGBoost model (Fig. 4).

The bar plot of mean absolute SHAP values ranked the importance of each predictor, revealing that the CK/CKMB ratio, AST, and InvasiveVent were the top three contributors to model predictions (Fig. 4A). The beeswarm plot further demonstrated the distribution of SHAP values across individual patients, where higher values of CK/CKMB ratio, AST, and LDH were strongly associated with increased risk of rhabdomyolysis, while higher albumin and phosphorus levels contributed negatively to risk prediction (Fig. 4B).

Individual-level explanations were provided through waterfall plots. For a representative RM patient, positive SHAP values from protective variables such as higher albumin offset the contributions from risk factors, shifting the prediction probability toward a low risk outcome (baseline expectation E[f(X)] = 0.758; model output f(x) = 0.957) (Fig. 4C). Conversely, for a representative non-RM patient, elevated CK/CKMB ratio, AST, and

requirement of invasive ventilation exerted strong positive SHAP contributions, driving the model prediction toward high risk of rhabdomyolysis (baseline expectation E[f(X)] = 0.242; model output f(x) = 0.043) **(**Fig. 4D**)**.

These findings indicate that the XGBoost model not only achieves high predictive performance but also provides clinically interpretable insights into the relative contribution of key laboratory markers and treatment variables.

Discussion

RM is a life-threatening complication in ICU patients with sepsis, as it exacerbates systemic inflammation, induces acute kidney injury (AKI) via myoglobin-mediated tubular damage, and significantly increases hospital mortality[14,15]. In our study, AKI incidence was significantly higher in patients with RM than in non-RM patients, reflecting the bidirectional pathophysiological link between RM and AKI in sepsis. Mechanistically, myoglobin released during RM-induced skeletal muscle necrosis directly causes renal tubular obstruction, oxidative stress, and inflammation—effects that combined with sepsis-related renal ischemia, exacerbate kidney dysfunction[2,16]; conversely, preexisting AKI impairs myoglobin and cytokine clearance, amplifying muscle necrosis and forming a vicious cycle[17]. Clinically, this comorbidity correlates with longer ICU stays (5.99 days in RM vs. 4.67 days in non-RM patients), highlighting the need for prioritized renal monitoring in RM patients. The RM group patients experienced more frequent invasive ventilation (83.61% vs. 55.27%) and CRRT (21.12% vs. 12.63%), indicating that RM might drive advanced organ support, showing the needs for integrated assessment of muscle injury and renal function in septic patients.

Several studies have focused on predicting outcomes in patients with RM[18,19], however, there are few studies investigating the prediction of the occurrence of rhabdomyolysis. Traditional RM prediction relies on single biomarkers (e.g., CK) with limited early sensitivity, and no tailored risk stratification tools exist for septic populations[20]. To address this gap, we developed an interpretable machine learning model for RM prediction in ICU septic patients, with the XGBoost model emerging as the optimal approach. This model achieved an AUC of 0.924 (95% CI: 0.907–0.941) and a Brier score of 0.90 in the testing set, outperforming logistic regression and other machine learning algorithms (e.g., random forest, ANN). DCA further confirmed its clinical utility, as it provided higher net benefits across a wide threshold probability range (0.1–0.8) compared to "treat all" or "treat none" strategies—critical for guiding targeted interventions and optimizing ICU resource allocation.

The SHAP analysis identified CK-CKMB ratio, AST, and InvasiveVent as the top three predictors of RM-findings that supported by both pathophysiological mechanisms and existing literature. The CK-CKMB ratio stood out as the most influential predictor of RM. Notably, RM is clinically defined by an acute increase in serum CK to more than five times the upper normal limit, with myocardial infarction excluded based on a CK-MB fraction < 5%[21]. Aligning with this diagnostic framework, our data showed a 4.8-fold higher ratio in RM versus non-RM patients (111 vs. 23 U/L, P < 0.001), indicating that higher CK-CKMB ratio is associated with increased skeletal muscle injury. There is observational and experimental data demonstrating that AST can be elevated in patients with RM due to muscle release of these enzymes[22], Liver failure was more common for intense RM patients[23]. In addition, sepsis could induce liver injury in any stage, and liver dysfunction is one of the hallmarks of the progressive development of sepsis into multi-organ dysfunction[24]. These studies could explain the elevation of AST in sepsis patients with RM. Notably, our study also found that elevated AST (117 vs. 40 U/L, P < 0.001) serve as indirect markers of skeletal muscle damage. However, whether there is an interaction between the liver and skeletal muscle during the development of rhabdomyolysis requires further basic research to confirm. Diaphragm biopsy specimens obtained from mechanically ventilated patients exhibit significant inflammatory infiltration and sarcomeric disarray—pathological features that closely resemble those observed in animal models of load-induced muscle injury[25,26]. Notably, high levels of respiratory effort are frequently documented in mechanically ventilated patients; this phenomenon is primarily driven by elevated respiratory drive, insufficient ventilator support, and episodes of patient–ventilator dyssynchrony. Collectively, these factors suggest that critically ill patients undergoing mechanical ventilation are at substantial risk of developing load-induced diaphragm injury[27]. Similarly, our study showed that the proportion of patients requiring InvasiveVent was significantly higher in the RM group than in the non-RM group. However, whether InvasiveVent directly contributes to RM via ventilator-induced diaphragm injury or disuse atrophy requires further basic and clinical research to be validated. Interestingly, SHAP analysis showed the negative contribution of InvasiveVent to RM prediction, indicating that InvasiveVent itself may confer indirect benefits via improved organ perfusion.

This study advances existing knowledge in three key ways. First, it is the first to develop an machine learning-based RM prediction model specifically for ICU septic patients, whereas previous studies focused on narrow subgroups such as trauma and drug-induced RM[28,29]. Our large sample size (3782 patients from the MIMIC database) and multi-method feature selection (univariate analysis, Lasso, Boruta) enhance the model's robustness and generalizability. Second, the emphasis on model interpretability via SHAP addresses a major limitation of "black-box" machine learning models in clinical practice: we not only identified key predictors but also quantified their individual contributions (e.g., a CK-CKMB ratio of 111 U/L increases RM probability by ~ 5%), facilitating clinician trust and adoption[30]. Third, the XGBoost model's ability to capture non-linear interactions outperforms traditional linear models, which often fail to account for the complex crosstalk between inflammation and organ dysfunction in sepsis[31].

This study has several limitations. First, due to the lack of an independent external cohort, we only performed internal validation through training/testing set splitting. This may restrict the model's generalizability to other ICU populations, such as those in European or Asian settings where sepsis management protocols differ[32,33]. Second, the retrospective design led to missing data on critical variables—including myoglobin levels (a direct marker of RM) and sepsis etiology, such as whether infections were bacterial or viral. The inclusion of these variables could have potentially improved the model's predictive performance. Third, the model was developed solely based on baseline admission data and did not incorporate dynamic changes in biomarkers (e.g., serial creatine kinase measurements) or clinical interventions like fluid resuscitation. Such dynamic information is critical for real-time assessment of rhabdomyolysis risk in clinical practice. Finally, we were unable to establish a causal relationship between certain predictors (e.g., InvasiveVent) and RM. This is because InvasiveVent may reflect the severity of sepsis rather than act as a direct cause of muscle injury.

In conclusion, we developed a highly performant and interpretable XGBoost model to predict RM in ICU septic patients, using readily available clinical variables (CK-CKMB ratio, AST, InvasiveVent) that facilitate seamless clinical implementation. Future studies should focus on external validation in multi-center prospective cohorts, integrating dynamic biomarkers (e.g., serial myoglobin) to develop real-time prediction tools, and conducting randomized controlled trials to verify whether model-guided interventions reduce RM-related AKI and mortality. With further refinement, this model has the potential to become a standard tool for early RM risk stratification in septic patients, improving clinical decision-making and patient outcomes.

Abbreviations

AKI
Acute kidney injury
AMI
Acute myocardial infarction
ANN
Artificial neural network
AUC
Area under the receiver operating characteristic curve
CHF
Congestive heart failure
CK
Creatine kinase
CKD
Chronic kidney disease
CLF
Chronic liver failure
CPR
Cardiopulmonary resuscitation
CRF
Chronic renal failure
CRRT
Continuous renal replacement therapy
ICU
Intensive care unit
DCA
Decision curve analysis
DM
Dermatomyositis
InvasiveVent
Invasive mechanical ventilation
LASSO
Least absolute shrinkage and selection operator
MIMIC-IV
Intensive Care IV
PM
Polymyositis
RM

Rhabdomyolysis
RRT
Renal replacement therapy
SE
Standard error
SHAP
Shapley Additive Explanations
SOFA
Sequential Organ Failure Assessment
SVM
Support vector machine
XGBoost
Extreme gradient boosting

Declarations

Submission declaration and verification

The work described has not been published previously, and is not under consideration for publication elsewhere.

Ethics approval and consent to participate

This retrospective study utilized data from the publicly available MIMIC-IV database. The requirement for ethical approval and informed consent was waived by the Institutional Review Board of Tianjin Medical University General Hospital. The study was conducted in accordance with the Declaration of Helsinki. Access to the MIMIC-IV database was granted after completing the required Collaborative Institutional Training Initiative (CITI) course.

Consent for publication

All the authors have consented to the publication of this research.

Availability of data and materials

The datasets used and/or analyzed during the current study are available from the corresponding author on reasonable request.

Competing interests

The authors declare that they have no competing interests.

Funding

This study was supported by the Science and Technology Commission of Chongqing (No.0202czzx2106), National Natural Science Foundation of China (No.82502660).

Clinical trial number

Not applicable.

Author contributions statement

Daqian Gu gave the study concept and design; Hongbin Deng drafted the manuscript; Xiangyi Zhou carried out the statistical analysis; Fachun Zhou supervised the study; all authors read and approved the final manuscript.

Acknowledgments

None.

References

1. Singer M, Deutschman CS, Seymour CW, et al. The Third International Consensus Definitions for Sepsis and Septic Shock (Sepsis-3). JAMA. 2016;315(8):801–10.
2. Torres PA, Helmstetter JA, Kaye AM, Kaye AD. Rhabdomyolysis: pathogenesis, diagnosis, and treatment. Ochsner J. 2015;15(1):58–69.

3. Rawson ES, Clarkson PM, Tarnopolsky MA. Perspectives on exertional rhabdomyolysis. Sports Med. 2017;47(Suppl 1):33–49.
4. Rout P, Chippa V, Adigun R. Rhabdomyolysis. *StatPearls*. Treasure Island (FL) ineligible companies. Disclosure: Venu Chippa declares no relevant financial relationships with ineligible companies. Disclosure: Rotimi Adigun declares no relevant financial relationships with ineligible companies.: StatPearls Publishing Copyright © 2025. StatPearls Publishing LLC.; 2025.
5. Nedel W, Deutschendorf C, Portela LVC. Sepsis-induced mitochondrial dysfunction: A narrative review. World J Crit Care Med. 2023;12(3):139.
6. Hu D, Sheeja Prabhakaran H, Zhang Y-Y, Luo G, He W, Liou Y-C. Mitochondrial dysfunction in sepsis: mechanisms and therapeutic perspectives. Crit Care. 2024;28(1):292.
7. Sun J, Zhang J, Tian J, et al. Mitochondria in sepsis-induced AKI. J Am Soc Nephrol. 2019;30(7):1151–61.
8. Tomašev N, Glorot X, Rae JW, et al. A clinically applicable approach to continuous prediction of future acute kidney injury. Nature. 2019;572(7767):116–9.
9. Henry KE, Hager DN, Pronovost PJ, Saria S. A targeted real-time early warning score (TREWScore) for septic shock. Sci Transl Med. 2015;7(299):ra299122–299122.
10. Goh KH, Wang L, Yeow AYK, et al. Artificial intelligence in sepsis early prediction and diagnosis using unstructured data in healthcare. Nat Commun. 2021;12(1):711.
11. Desautels T, Calvert J, Hoffman J, et al. Prediction of sepsis in the intensive care unit with minimal electronic health record data: a machine learning approach. JMIR Med Inf. 2016;4(3):e5909.
12. Hou N, Li M, He L, et al. Predicting 30-days mortality for MIMIC-III patients with sepsis-3: a machine learning approach using XGboost. J translational Med. 2020;18(1):462.
13. Zhang Y, Xu W, Yang P, Zhang A. Machine learning for the prediction of sepsis-related death: a systematic review and meta-analysis. BMC Med Inf Decis Mak. 2023;23(1):283.
14. Wang Z, Wang Q, Chen J, Cai L. Rhabdomyolysis in intensive care unit—distinctive clinical indicators and prognosis. BMC Anesthesiol. 2025;25(1):84.
15. Miyauchi H, Okubo K, Iida K, et al. Multiple site inflammation and acute kidney injury in crush syndrome. Front Pharmacol. 2024;15:1458997.
16. Bellomo R, Kellum JA, Ronco C, et al. Acute kidney injury in sepsis. Intensive Care Med. 2017;43(6):816–28.
17. Zhou X, Yang Y, Li P, Wang F, Zhang L, Fu P. Efficacy of haemoadsorption combined with continuous renal replacement therapy in patients with rhabdomyolysis and acute kidney injury: a retrospective study. Clin kidney J. 2025;18(2):sfae406.
18. Liu C, Liu X, Mao Z, et al. Interpretable machine learning model for early prediction of mortality in ICU patients with rhabdomyolysis. Med Sci Sports Exerc. 2021;53(9):1826–34.
19. Liu C, Shi J, Wang F et al. Development and validation of an interpretable multi-task model to predict outcomes in patients with rhabdomyolysis: a multicenter retrospective cohort study. EClinicalMedicine 2025;87.
20. Lippi G, Schena F, Ceriotti F. Diagnostic biomarkers of muscle injury and exertional rhabdomyolysis. Clin Chem Lab Med (CCLM). 2018;57(2):175–82.
21. Lane R, Phillips M. Rhabdomyolysis. In. Vol 327: British Medical Journal Publishing Group; 2003:115–116.
22. Lim AK. Abnormal liver function tests associated with severe rhabdomyolysis. World J Gastroenterol. 2020;26(10):1020.
23. Martinez T, Liaud-Laval G, Laitselart P, et al. Study of the relationship between liver function markers and traumatic rhabdomyolysis: a retrospective study of hemorrhagic patients admitted to intensive care unit in a level I trauma center. Anesth Analgesia. 2023;136(5):842–51.
24. Liu Z, Yuan X, Huang Y et al. The role of interferon-induced proteins with tetratricopeptide repeats 1 and 2 in Sepsis-induced acute liver injury. Infect Drug Resist 2024:2337–49.
25. Van den Berg M, Hooijman PE, Beishuizen A, et al. Diaphragm atrophy and weakness in the absence of mitochondrial dysfunction in the critically ill. Am J Respir Crit Care Med. 2017;196(12):1544–58.
26. Jaber S, Petrof BJ, Jung B, et al. Rapidly progressive diaphragmatic weakness and injury during mechanical ventilation in humans. Am J Respir Crit Care Med. 2011;183(3):364–71.
27. Schreiber A, Bertoni M, Goligher EC. Avoiding respiratory and peripheral muscle injury during mechanical ventilation: diaphragm-protective ventilation and early mobilization. Crit Care Clin. 2018;34(3):357–81.
28. Tarazona V, Figueiredo S, Hamada S, et al. Admission serum myoglobin and the development of acute kidney injury after major trauma. Ann Intensiv Care. 2021;11(1):140.
29. Yamanaka T, Takemura K, Hayashida M, Suyama K, Urakami S, Miura Y. Cabozantinib-induced serum creatine kinase elevation and rhabdomyolysis: a retrospective case series. Cancer Chemother Pharmacol. 2023;92(3):235–40.
30. Huang D, Gong L, Wei C, Wang X, Liang Z. An explainable machine learning-based model to predict intensive care unit admission among patients with community-acquired pneumonia and connective tissue disease. Respir Res. 2024;25(1):246.

31. Li X, Wu R, Zhao W, et al. Machine learning algorithm to predict mortality in critically ill patients with sepsis-associated acute kidney injury. Sci Rep. 2023;13(1):5223.
32. Gildea A, Mulvihill C, McFarlane E, Gray A, Singer M. Recognition, diagnosis, and early management of suspected sepsis: summary of updated NICE guidance. BMJ 2024;385.
33. Mehta Y, Paul R, Rabbani R, Acharya SP, Withanaarachchi UK. Sepsis management in Southeast Asia: a review and clinical experience. J Clin Med. 2022;11(13):3635.

Tables

Table 1 Baseline characteristics and comparison between RM and non-RM in MIMIC database

Demographic characteristics	Overall n=3782	Non-RM n=2873	RM n=909	P value
Demographic information				
Male gender, n (%)	2148 [56.80]	1504 [52.35]	644 [70.85]	<0.001
Age(yd)	65.00 [55.00, 75.00]	67.00 [57.00, 76.00]	58.00 [49.00, 69.00]	<0.001
Height (cm)	170.00 [163.00, 178.00]	168.00 [163.00, 175.00]	173.00 [165.00, 178.00]	<0.001
Weight (kg)	79.00 [67.00, 94.50]	77.20 [65.50, 92.30]	84.60 [71.90, 98.60]	<0.001
BMI (kg/m^2)	27.47 [23.73, 32.03]	27.21 [23.44, 31.74]	28.41 [24.93, 32.86]	<0.001
Los_hospital (d)	16.76 [9.60, 27.80]	17.96 [10.04, 29.28]	13.61 [7.56, 22.71]	<0.001
Los_icu (d)	4.91 [2.44, 10.23]	4.67 [2.28, 9.84]	5.99 [2.84, 11.70]	<0.001
Severity of illness				
AKI_score (median [IQR])	2.00 [2.00, 3.00]	2.00 [2.00, 3.00]	2.00 [2.00, 3.00]	0.005
Apsiii (median [IQR])	54.00 [42.00, 67.00]	54.00 [43.00, 67.00]	53.00 [40.00, 69.00]	0.542
SAPSii (median [IQR])	41.00 [33.00, 50.00]	41.00 [33.00, 49.00]	40.00 [31.00, 51.00]	0.266
SOFA (median [IQR])	7.00 [5.00, 11.00]	7.00 [5.00, 10.00]	8.00 [6.00, 12.00]	<0.001
GCS (median [IQR])	13.00 [9.00, 14.00]	13.00 [10.00, 14.00]	13.00 [9.00, 14.00]	0.002
SIRS (median [IQR])	3.00 [2.00, 4.00]	3.00 [2.00, 3.00]	3.00 [3.00, 4.00]	<0.001
LODS (median [IQR])	6.00 [4.00, 8.00]	6.00 [4.00, 8.00]	6.00 [4.00, 8.00]	<0.001
Charlson (median [IQR])	5.00 [3.00, 7.00]	6.00 [4.00, 7.00]	3.00 [1.00, 6.00]	<0.001
MELD (median [IQR])	17.58 [10.00, 24.68]	18.00 [11.00, 25.00]	16.57 [10.00, 24.00]	0.038
OASIS (median [IQR])	35.00 [30.00, 40.00]	35.00 [29.00, 40.00]	36.00 [31.00, 42.00]	<0.001
Vital signs				<0.001
Temperature (°C)	37.39 [37.00, 37.94]	37.28 [37.00, 37.83]	37.70 [37.20, 38.28]	0.002
HR (bpm)	109.00 [96.00, 122.00]	108.00 [96.00, 121.00]	111.00 [98.00, 122.00]	0.045
RR (bpm)	28.75 [25.00, 33.00]	29.00 [25.00, 33.00]	28.00 [24.00, 32.00]	<0.001
SBP (mmHg)	144.00 [130.00, 158.00]	143.00 [129.00, 157.00]	146.00 [134.00, 162.00]	<0.001
DBP (mmHg)	84.00 [73.00, 96.00]	84.00 [73.00, 96.00]	85.00 [76.00, 97.00]	<0.001
MBP (mmHg)	99.75 [89.00, 112.00]	99.00 [88.00, 111.00]	103.00 [93.00, 116.00]	0.542
Laboratory fndings				
Spo2 (%)	100.00 [100.00, 100.00]	100.00 [100.00, 100.00]	100.00 [100.00, 100.00]	0.037
Calcium_free (mmol/L)	1.13 [1.08, 1.19]	1.13 [1.08, 1.19]	1.14 [1.08, 1.20]	0.007
WBC (K/uL)	12.70 [8.70, 17.80]	12.30 [8.30, 17.60]	13.50 [10.00, 18.40]	<0.001
Hematocrit %	31.80 [28.20, 36.00]	30.90 [27.70, 34.80]	34.60 [31.10, 38.60]	<0.001
MCH (pg)	30.50 [28.90, 31.90]	30.40 [28.70, 31.80]	30.70 [29.40, 32.00]	<0.001
MCV (fL)	93.00 [88.00, 97.00]	93.00 [88.00, 98.00]	92.00 [88.00, 96.00]	0.005
MCHC (%)	33.20 [32.00, 34.30]	32.90 [31.90, 34.10]	33.90 [32.70, 34.90]	<0.001
RDW (%)	15.60 [14.30, 17.10]	16.00 [14.60, 17.50]	14.70 [13.70, 15.60]	<0.001
PLT (K/uL)	189.00 [125.00, 258.00]	190.00 [121.00, 261.00]	188.00 [139.00, 248.00]	0.451
RBC (m/uL)	3.48 [3.05, 3.98]	3.37 [2.97, 3.85]	3.80 [3.39, 4.26]	<0.001
Alb (g/dl)	2.90 [2.60, 3.30]	2.90 [2.50, 3.30]	3.10 [2.70, 3.40]	<0.001
Creatinine (mg/dl)	1.30 [0.90, 2.30]	1.30 [0.80, 2.20]	1.50 [1.00, 2.40]	<0.001

BUN (mg/dl)	28.00 [17.00, 43.00]	29.00 [18.00, 45.00]	25.00 [16.00, 38.00]	<0.001
Aniongap	16.00 [13.00, 19.00]	16.00 [13.00, 18.00]	17.00 [14.00, 20.00]	<0.001
PT (seconds)	15.30 [13.30, 19.10]	15.50 [13.30, 19.50]	14.90 [13.00, 17.90]	<0.001
PTT (seconds)	33.50 [28.70, 42.48]	33.70 [28.90, 42.30]	32.70 [28.30, 42.90]	0.139
INR	1.40 [1.20, 1.80]	1.40 [1.20, 1.80]	1.30 [1.20, 1.70]	<0.001
CK_CKMB_ratio (U/L)	33.00 [14.00, 92.00]	23.00 [11.00, 54.00]	111.00 [57.00, 210.00]	<0.001
ALT (U/L)	33.00 [18.00, 75.75]	29.00 [16.00, 60.00]	58.00 [29.00, 161.00]	<0.001
AST (U/L)	50.00 [27.00, 120.00]	40.00 [24.00, 84.00]	117.00 [54.00, 335.00]	<0.001
ALP (U/L)	88.00 [62.00, 133.00]	95.00 [67.00, 142.00]	66.00 [49.00, 95.00]	<0.001
Bilirubin_total (mg/dl)	0.80 [0.40, 1.70]	0.80 [0.40, 1.80]	0.70 [0.40, 1.40]	<0.001
LDH (U/L)	308.00 [218.00, 477.00]	277.00 [205.00, 408.00]	453.00 [302.00, 702.00]	<0.001
Chloride (mg/dl)	106.00 [102.00, 110.00]	105.00 [101.00, 110.00]	108.00 [104.00, 112.00]	<0.001
Glucose (mg/dl)	155.50 [121.00, 204.00]	150.00 [119.00, 198.00]	171.00 [132.00, 224.00]	<0.001
Bicarbonate (g/dl)	24.00 [21.00, 26.00]	24.00 [21.00, 27.00]	23.00 [21.00, 26.00]	<0.001
Hb (g/dl)	10.50 [9.20, 11.90]	10.10 [8.90, 11.40]	11.70 [10.40, 12.90]	<0.001
K (mEq/L)	4.40 [4.00, 4.90]	4.30 [4.00, 4.80]	4.60 [4.10, 5.20]	<0.001
Na (mEq/L)	140.00 [137.00, 143.00]	139.00 [136.00, 142.00]	141.00 [138.00, 144.00]	<0.001
Mg (mg/dL)	2.20 [1.90, 2.40]	2.20 [1.90, 2.40]	2.20 [2.00, 2.50]	<0.001
Ca(mg/dL)	8.40 [7.90, 8.80]	8.40 [7.90, 8.90]	8.30 [7.90, 8.70]	<0.001
P (mg/dL)	4.10 [3.30, 5.10]	4.00 [3.20, 4.90]	4.40 [3.50, 5.40]	<0.001
Input_24h_sum (ml)	4964.50 [2649.00, 8077.00]	4255.00 [2301.00, 7067.00]	7327.00 [4617.00, 10827.00]	<0.001
Output_24h_sum (ml)	1860.00 [1050.00, 3033.75]	1770.00 [994.00, 2810.00]	2340.00 [1306.50, 3580.00]	<0.001
Output_urine_sum (ml)	1302.50 [743.50, 2050.00]	1270.00 [729.00, 1975.00]	1430.00 [830.00, 2240.00]	<0.001
Comorbidity, n (%)				
Smoker (%)	328 (8.67)	252 (8.77)	76 (8.36)	0.752
Alcohol_abuse (%)	59 (1.56)	41 (1.43)	18 (1.98)	0.308
Hypertension (%)	1391 (36.78)	1046 (36.41)	345 (37.95)	0.422
Diabetes (%)	1204 (31.84)	978 (34.04)	226 (24.86)	<0.001
Myocardial_infarct (%)	279 (7.38)	224 (7.80)	55 (6.05)	0.092
Congestive_heart_failure (%)	1230 (32.52)	1026 (35.71)	204 (22.44)	<0.001
Mild_liver_disease (%)	890 (23.53)	697 (24.26)	193 (21.23)	0.067
Severe_liver_disease (%)	472 (12.48)	426 (14.83)	46 (5.06)	<0.001
Renal_disease (%)	1016 (26.86)	856 (29.79)	160 (17.60)	<0.001
Chronic_pulmonary_disease (%)	1059 (28.00)	836 (29.10)	223 (24.53)	0.009
Cerebrovascular_disease (%)	550 (14.54)	405 (14.10)	145 (15.95)	0.184
Peripheral_vascular_disease (%)	504 (13.33)	373 (12.98)	131 (14.41)	0.294
Dementia (%)	123 (3.25)	105 (3.65)	18 (1.98)	0.018
Peptic_ulcer_disease (%)	162 (4.28)	140 (4.87)	22 (2.42)	0.002
Paraplegia (%)	197 (5.21)	146 (5.08)	51 (5.61)	0.589
Malignant_cancer (%)	578 (15.28)	509 (17.72)	69 (7.59)	<0.001
Metastatic_solid_tumor (%)	179 (4.73)	151 (5.26)	28 (3.08)	0.009

Aids (%)	41 (1.08)	30 (1.04)	11 (1.21)	0.812
Rheumatic_disease (%)	171 (4.52)	144 (5.01)	27 (2.97)	0.013
AKI (%)	3224 (85.25)	2422 (84.30)	802 (88.23)	0.004
Treatment status				
InvasiveVent (%)	2348 (62.08)	1588 (55.27)	760 (83.61)	<0.001
CPR (%)	76 (2.01)	45 (1.57)	31 (3.41)	0.001
CRRT (%)	555 (14.67)	363 (12.63)	192 (21.12)	<0.001
RRT (%)	772 (20.41)	544 (18.93)	228 (25.08)	<0.001

Data are shown as median with interquartile range (IQR) for continuous variables and number with percentage for categorical variables

SOFA: Sequential Organ Failure Assessment, SAPSII: Simplified Acute Physiology Score II, APSIII: Acute Physiology Score III, OASIS: Oxford Acute Severity of Illness Score, GCS: Glasgow Coma Scale, SIRS: Systemic Inflammatory Response Syndrome, LODS: Logistic Organ Dysfunction System, MELD: Model for End-Stage Liver Disease, Charlson: Charlson Comorbidity Index, RM: Rhabdomyolysis, BMI: Body Mass Index, HR: Heart Rate, RR: Respiratory Rate, SBP: Systolic Blood Pressure, DBP: Diastolic Blood Pressure, MBP: Mean Blood Pressure, SpO2: Oxygen Saturation, WBC: White Blood Cell, MCH: Mean Corpuscular Hemoglobin, MCV: Mean Corpuscular Volume, MCHC: Mean Corpuscular Hemoglobin Concentration, RDW: Red Cell Distribution Width, PLT: Platelet, RBC: Red Blood Cell, Alb: Albumin, BUN: Blood Urea Nitrogen, PT: Prothrombin Time, PTT: Partial Thromboplastin Time, INR: International Normalized Ratio, ALT: Alanine Aminotransferase, AST: Aspartate Aminotransferase, ALP: Alkaline Phosphatase, LDH: Lactate Dehydrogenase, Hb: Hemoglobin, AKI: Acute Kidney Injury, CPR: Cardiopulmonary Resuscitation, CRRT: Continuous Renal Replacement Therapy, RRT: Renal Replacement Therapy, IQR: Interquartile Range

Table 2 Performance of 6 machine learning-based models for predicting ICU admission in the validation set

Model	AUC	95% CI Lower	95% CI Upper	Accuracy	Precision	Sensitivity	Specificity	F1 Score	Kappa	Youden's J	PPV	NPV
Logistic	0.877	0.856	0.898	0.826	0.712	0.463	0.941	0.561	0.459	0.404	0.712	0.847
Decision Tree	0.886	0.864	0.907	0.853	0.709	0.662	0.914	0.684	0.589	0.576	0.709	0.895
Random Forest	0.911	0.891	0.930	0.876	0.799	0.643	0.949	0.713	0.635	0.592	0.799	0.894
XGBoost	0.924	0.907	0.941	0.883	0.791	0.695	0.942	0.740	0.664	0.637	0.791	0.907
SVM	0.885	0.866	0.905	0.825	0.720	0.445	0.945	0.550	0.449	0.390	0.720	0.844
ANN	0.911	0.893	0.929	0.865	0.772	0.621	0.942	0.688	0.603	0.563	0.772	0.887

AUC: area under the receiver operating characteristic curve; XGBoost: eXtreme gradient boosting; SVM: Support Vector Machine; ANN: Artificial Neural Network

Figures

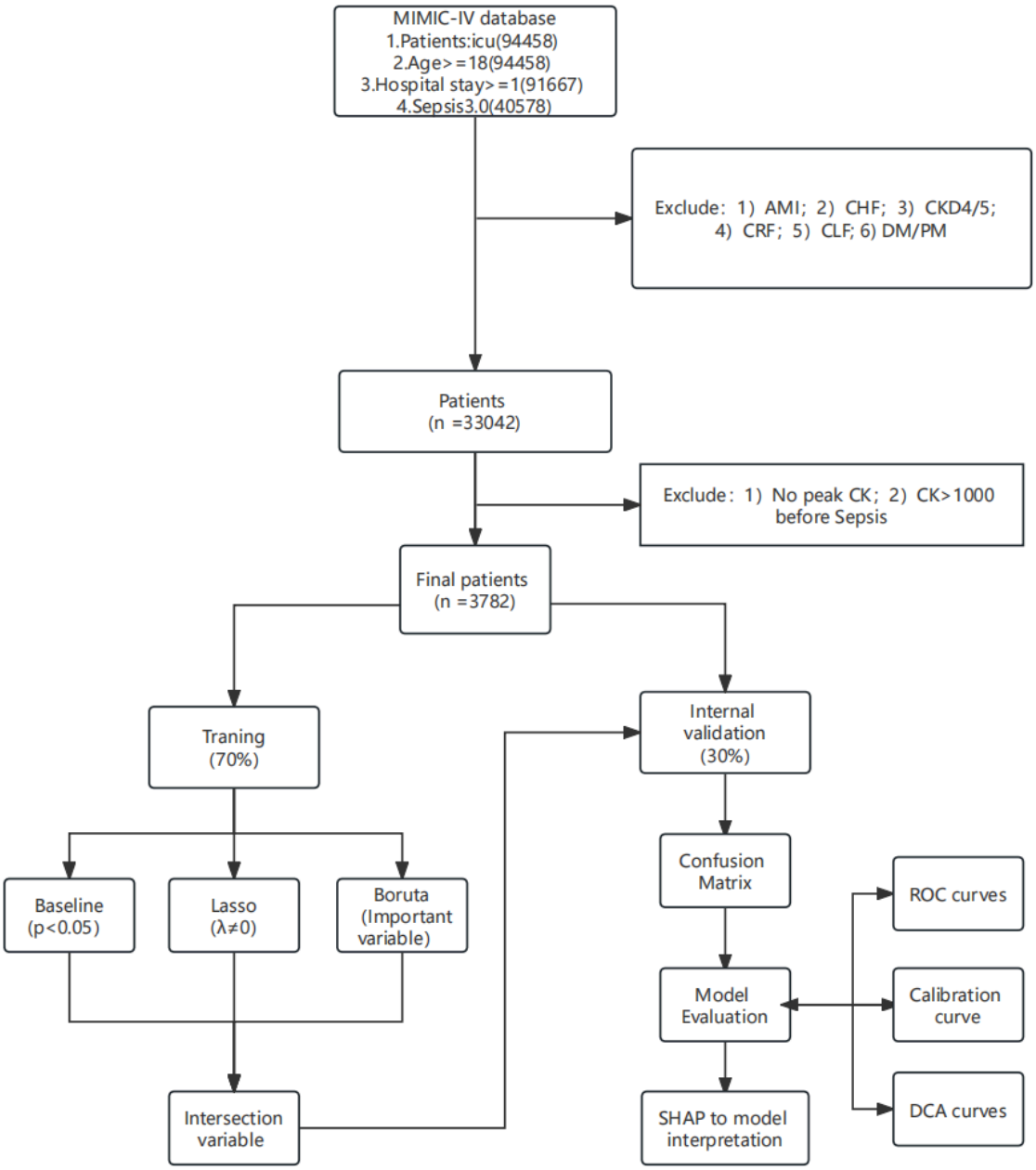


Figure 1

Flowchart of patient selection

RM: rhabdomyolysis; CK: creatine kinase; AMI: acute myocardial infarction; CHF: congestive heart failure; CKD: chronic kidney disease; CRF: chronic renal failure; CLF: chronic liver failure; DM: dermatomyositis; PM: polymyositis; SHAP: Shapley Additive explanation.

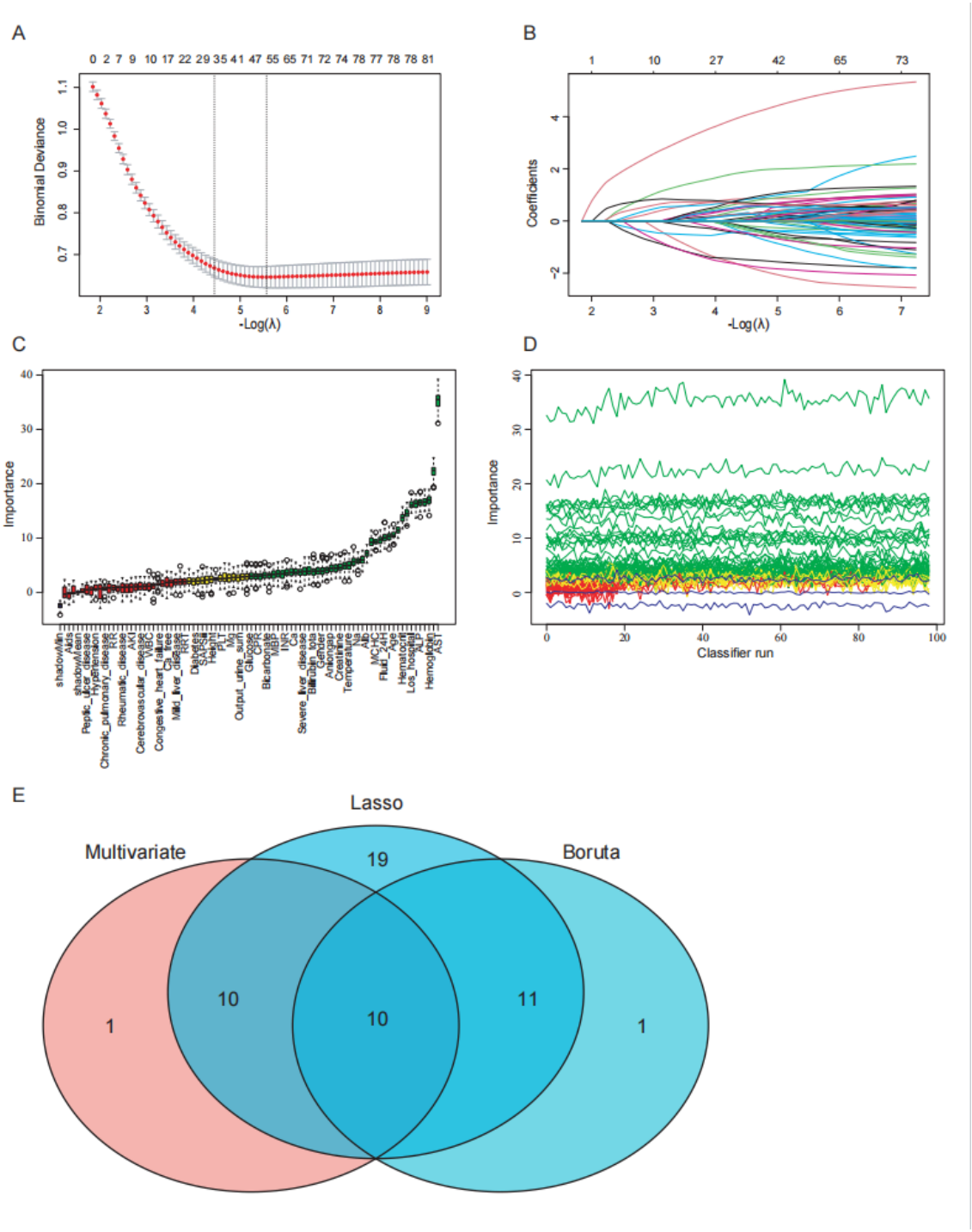


Figure 2

Features selected by Boruta, Lasso and univariate analysis.

A. The optimal lambda selection in the Lasso regression with 10-fold cross-validation. Misclassification errors of different variables against log(lambda) are revealed. The two vertical dashed lines represent the optimal value under the minimum criterion and 1-SE criterion, respectively. The "lambda" is the tuning parameter. A total of 33 predictors with non-zero coefficients are identified. **B.** The Lasso regression coefficient profiles of all baseline characteristics. **C.** Variables selected by Boruta algorithm. The minimum, average and maximum shadow score are shown in blue. **D.** In terms of the score of feature importance, the 22 variables in green are regarded as important variables, while yellow are neutral and red are rejected. **E.** The Venn diagram of features selected by Boruta, Lasso and univariate analysis. The intersection results of three methods yield 10 clinical characteristics. SE, standard error; Lasso, least absolute shrinkage and selection operator.

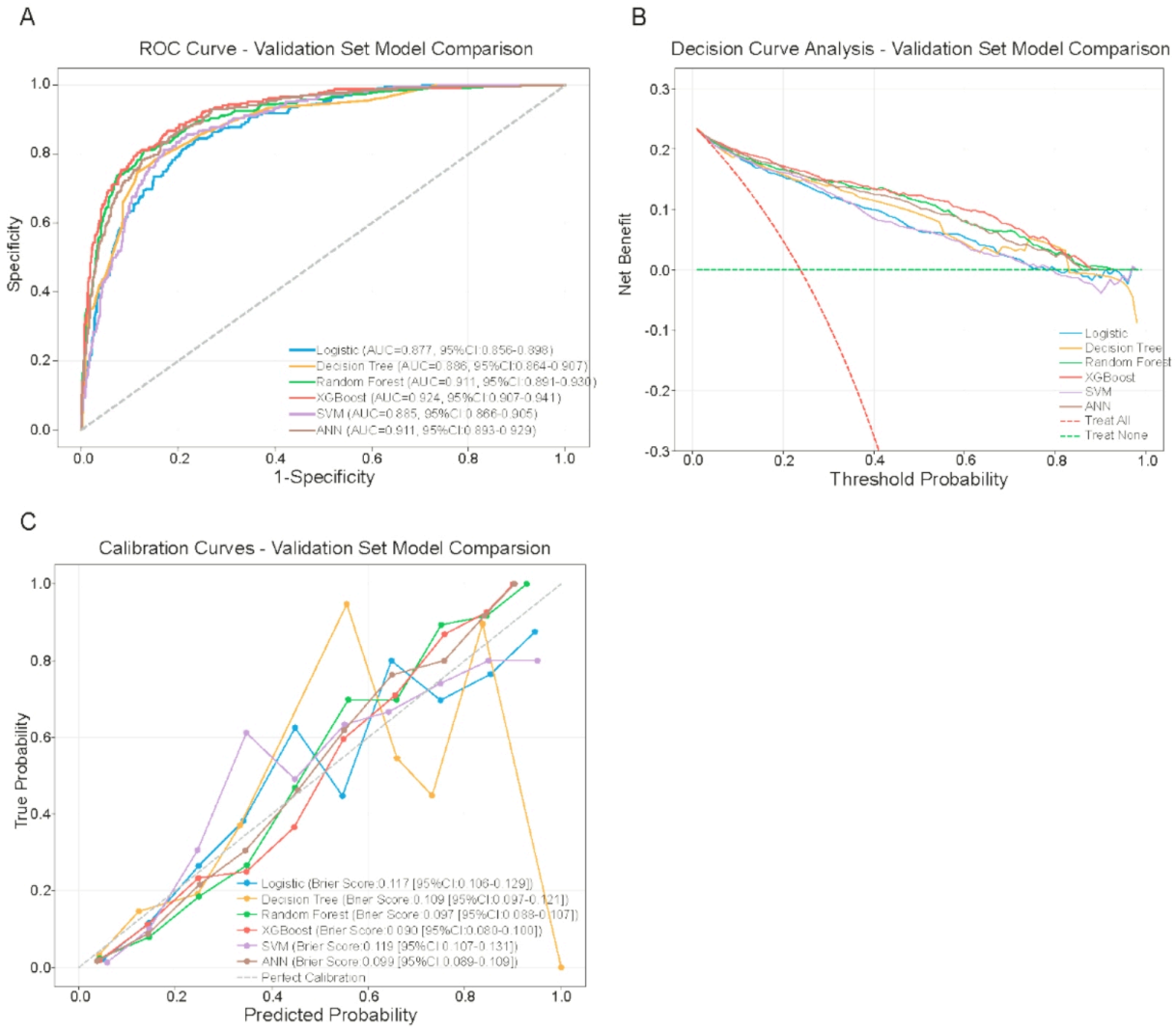


Figure 3

Performance evaluation of machine learning models for predicting clinical outcomes in the validation set.

(A) Calibration curves of six machine learning models with their Brier scores and 95% confidence intervals. The gray line represents perfect calibration. (B) Decision curve analysis showing the net benefit of each model across different threshold probabilities. The gray lines represent the strategies of treating all patients and treating none. (C) Receiver operating characteristic curves with area under the curve values and 95% confidence intervals for each model. AUC, area under the curve; CI, confidence interval; Logistic, logistic regression; Decision Tree, decision tree algorithm; Random Forest, random forest algorithm; XGBoost, extreme gradient boosting; SVM, support vector machine; ANN, artificial neural network.

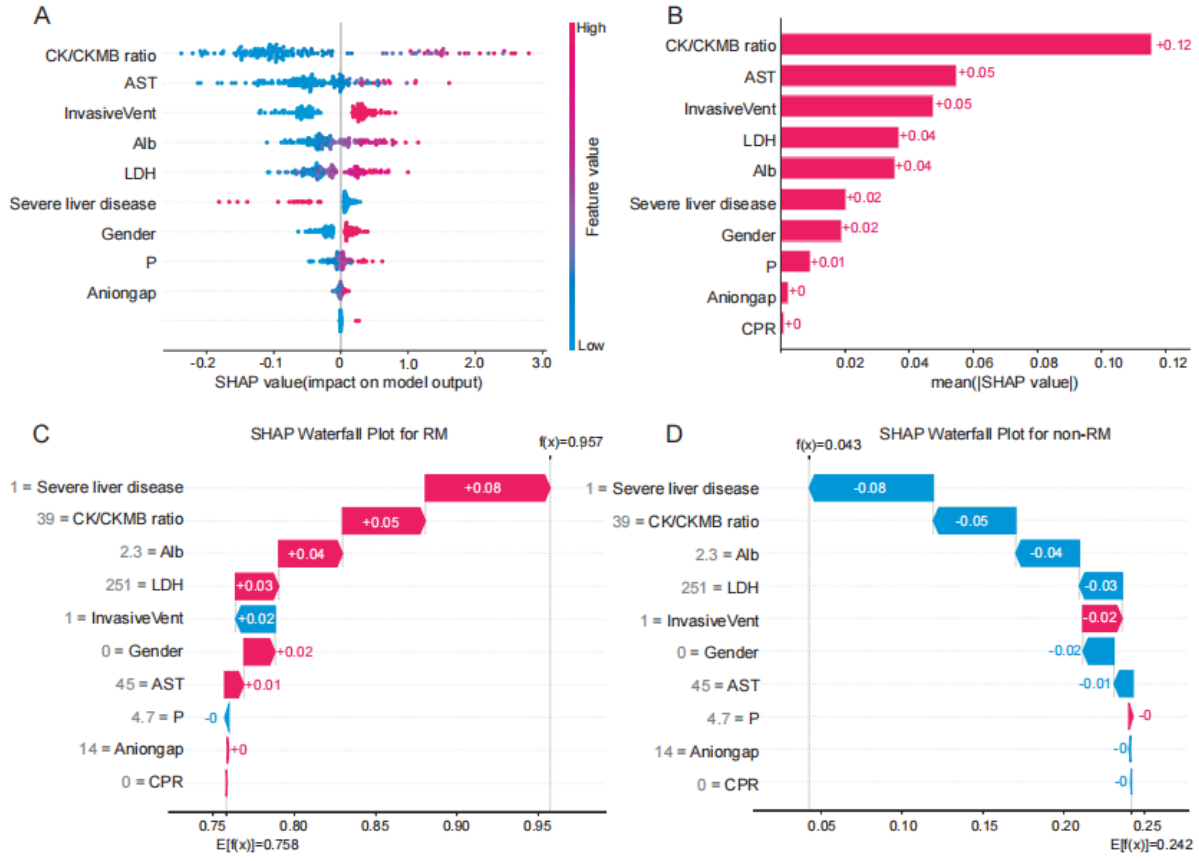


Figure 4

SHAP (Shapley Additive Explanations) analysis of the XGBoost model for predicting clinical outcomes.

(A) Bar plot showing the mean absolute SHAP values for each predictor in descending order of importance. CK/CKMB, AST, and InvasiveVent are the top three most important features. (B) Beeswarm plot displaying the distribution of SHAP values for each feature across all samples. Each point represents a single patient, with color indicating the feature value (red: low, blue: high). The horizontal dispersion shows the impact of each feature on model output. (C) Waterfall plot for a representative patient fromRM, showing how each feature contributes to the final prediction. The baseline expectation E[f(X)] is 0.758, while the model output f(x) is 0.957. (D) Waterfall plot for a representative patient from non-RM, with baseline expectation E[f(X)] of 0.242 and model output f(x) of 0.043. Positive SHAP values push the prediction higher, while negative values push it lower. SHAP, Shapley Additive Explanations; ICU, intensive care unit; CK/CKMB, creatine kinase and its MB isoenzyme ratio; AST, aspartate aminotransferase; LDH, lactate dehydrogenase; Alb, albumin; P, phosphorus; CPR, cardiopulmonary resuscitation.

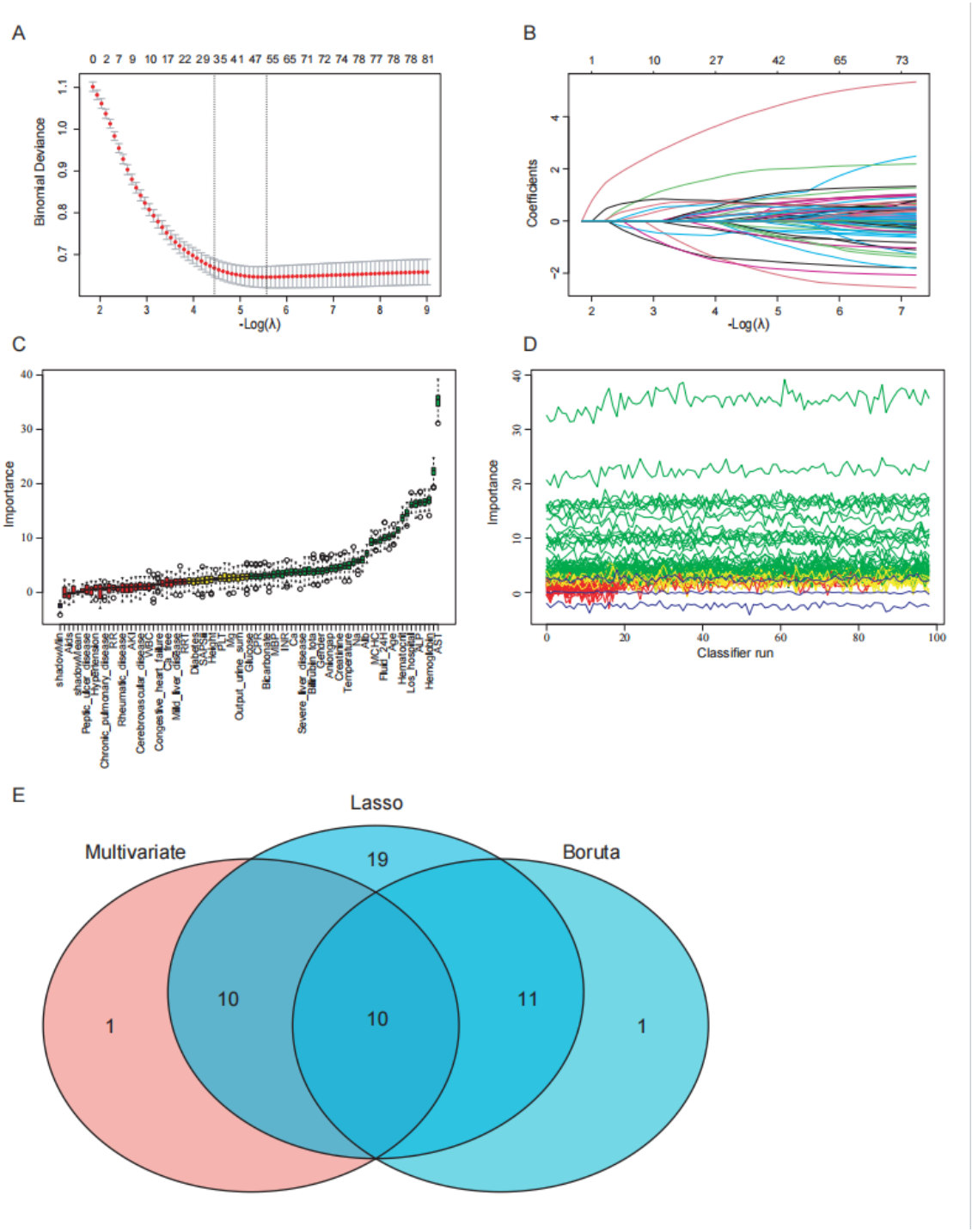


Figure 22

Features selected by Boruta, Lasso and univariate analysis.

A. The optimal lambda selection in the Lasso regression with 10-fold cross-validation. Misclassification errors of different variables against log(lambda) are revealed. The two vertical dashed lines represent the optimal value under the minimum criterion and 1-SE criterion, respectively. The "lambda" is the tuning parameter. A total of 33 predictors with non-zero coefficients are identified. **B.** The Lasso regression coefficient profiles of all baseline characteristics. **C.** Variables selected by Boruta algorithm. The minimum, average and maximum shadow score are shown in blue. **D.** In terms of the score of feature importance, the 22 variables in green are regarded as important variables, while yellow are neutral and red are rejected. **E.** The Venn diagram of features selected by Boruta, Lasso and univariate analysis. The intersection results of three methods yield 10 clinical characteristics. SE, standard error; Lasso, least absolute shrinkage and selection operator.

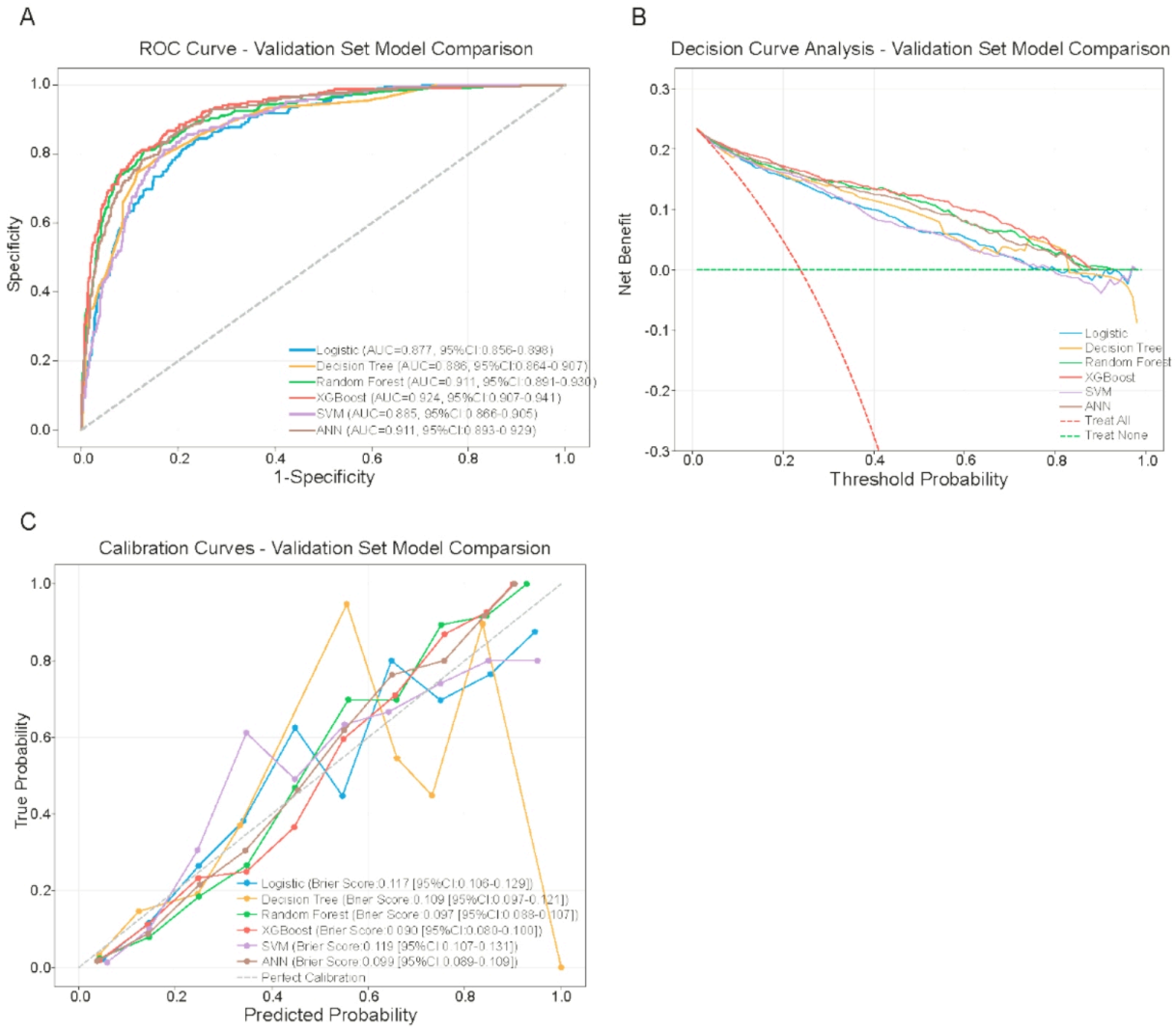


Figure 23

Performance evaluation of machine learning models for predicting clinical outcomes in the validation set.

(A) Calibration curves of six machine learning models with their Brier scores and 95% confidence intervals. The gray line represents perfect calibration. (B) Decision curve analysis showing the net benefit of each model across different threshold probabilities. The gray lines represent the strategies of treating all patients and treating none. (C) Receiver operating characteristic curves with area under the curve values and 95% confidence intervals for each model. AUC, area under the curve; CI, confidence interval; Logistic, logistic regression; Decision Tree, decision tree algorithm; Random Forest, random forest algorithm; XGBoost, extreme gradient boosting; SVM, support vector machine; ANN, artificial neural network.

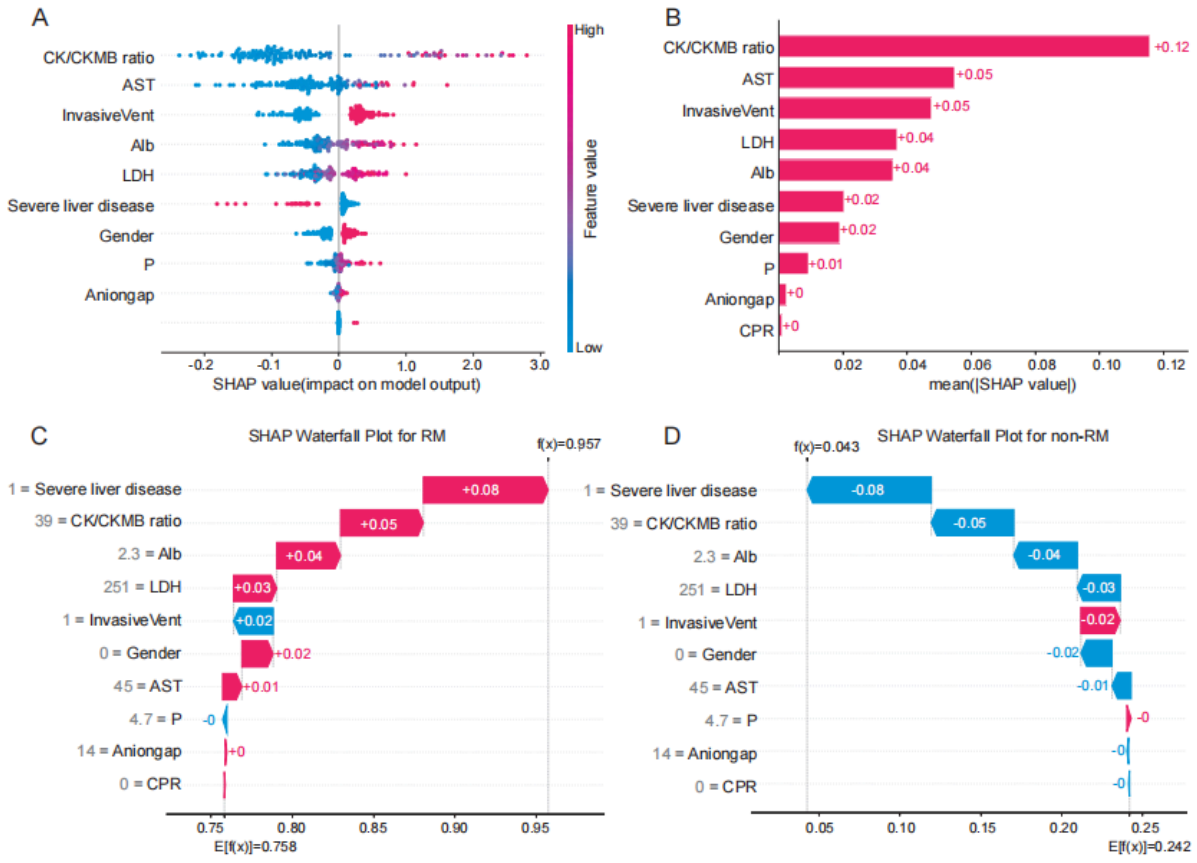


Figure 24

SHAP (Shapley Additive Explanations) analysis of the XGBoost model for predicting clinical outcomes.

(A) Bar plot showing the mean absolute SHAP values for each predictor in descending order of importance. CK/CKMB, AST, and InvasiveVent are the top three most important features. (B) Beeswarm plot displaying the distribution of SHAP values for each feature across all samples. Each point represents a single patient, with color indicating the feature value (red: low, blue: high). The horizontal dispersion shows the impact of each feature on model output. (C) Waterfall plot for a representative patient fromRM, showing how each feature contributes to the final prediction. The baseline expectation E[f(X)] is 0.758, while the model output f(x) is 0.957. (D) Waterfall plot for a representative patient from non-RM, with baseline expectation E[f(X)] of 0.242 and model output f(x) of 0.043. Positive SHAP values push the prediction higher, while negative values push it lower. SHAP, Shapley Additive Explanations; ICU, intensive care unit; CK/CKMB, creatine kinase and its MB isoenzyme ratio; AST, aspartate aminotransferase; LDH, lactate dehydrogenase; Alb, albumin; P, phosphorus; CPR, cardiopulmonary resuscitation.

Supplementary Files

This is a list of supplementary files associated with this preprint. Click to download.

- ANNconfusionmatrix.pdf
- Logisticconfusionmatrix.pdf
- SVMconfusionmatrix.pdf
- RandomForestconfusionmatrix.pdf
- DecisionTreeconfusionmatrix.pdf
- XGBoostconfusionmatrix.pdf
- file.docx
- file.xlsx
- file.pdf